Promotion of sugar–lectin recognition through the multiple sugar presentation offered by regioselectively addressable functionalized templates (RAFT): a QCM-D and SPR study†

Marie Wilczewski, Angéline Van der Heyden,* Olivier Renaudet, Pascal Dumy, Liliane Coche-Guérente and Pierre Labbé*

Received 22nd October 2007, Accepted 18th December 2007
First published as an Advance Article on the web 19th February 2008
DOI: 10.1039/b716214f

The investigation of recognition events between carbohydrates and proteins, especially the understanding of how spatial factors and binding avidity are correlated, remains a great interest for glycobiology. In this context we have investigated by nanogravimetry (QCM-D) and surface plasmon resonance (SPR), the kinetics and thermodynamics of the interaction between concanavalin A (Con A) and various neoglycopeptide ligands of low molecular weight. Regioselectively addressable functionalized templates (RAFT) have been used as scaffolds for the design of multivalent neoglycopeptides bearing thiol or biotin functions for their anchoring on transducer surfaces. Although these multivalent neoglycopeptide ligands cannot span multiple binding sites within the same Con A protein, they have increased activities relative to their monovalent counterpart. Our results emphasize that the multivalent RAFT ligands function by clustering several lectins, which leads to enhanced affinities.

Introduction

Lectin–carbohydrate interactions play a crucial role in the biomolecular interactions of various biological processes. These interactions are involved in inflammation processes, in cellular recognition including adhesion of infectious agents and the immune response.[1,2] Lectins, carbohydrate binding proteins, contain two or more specific sugar-combining sites and comprise a large family of recognition molecules, especially in the immune system. While the affinity between lectin and monosaccharides is weak, K_D in the 0.1–1 mM range, sugar–protein interactions are very efficient and specific due to multivalent events commonly known as the 'glycoside cluster effect".[3] This effect has previously been defined as an "affinity enhancement achieved by multivalent ligands over monovalent ones that is greater than would be expected from a simple effect of concentration increase".[4] Multivalent carbohydrate derivatives that can simultaneously interact with several binding sites of a multivalent lectin (chelating effect) are relevant for medicinal interest.[4] In this context, some small multivalent ligands, in which the distances between their carbohydrate moieties are too low to enable their binding to multiple sites of the same lectin, have proved to be also more efficient than monovalent ones.[5–7] This improvement could be attributed either to local ligand concentration effects, also defined as proximity/statistical effects[8,9] or, as rarely demonstrated, to a favorable clustering of lectins (interaction of one multivalent ligand with several lectins).[5] These various possibilities related to the "glycoside cluster effect" are shown pictorially in Fig. 1. In the last few years, we have developed new molecular tools that combine recognition and effector properties for diverse biological applications such as vectors for neo-vasculature targeting,[10] cell surface mimics,[11] anti-tumoral synthetic vaccines[12] or tumor imaging.[13] Our approach utilizes cyclodecapeptide templates based on the TASP model which were previously described for protein *de novo* design.[14] These topological templates (namely regioselectively addressable functionalized templates, "RAFT") exhibit two independent and

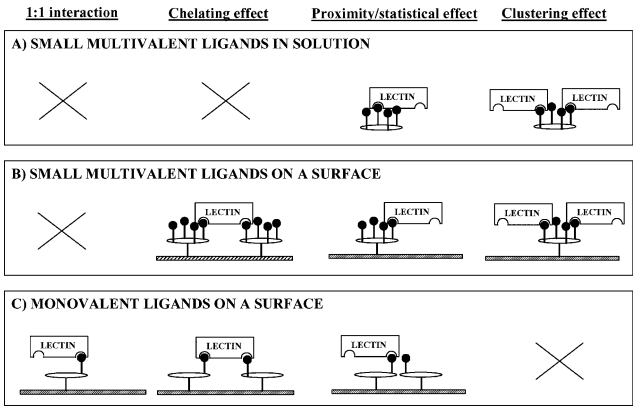

Fig. 1 Schematic representation of the three main effects at the origin of the "glycoside cluster effect", illustrated by the interaction of a bivalent lectin with small multivalent ligands which cannot span to multiple sites of a single lectin (A) in solution, (B) immobilized on a surface, and (C) comparison with the interaction of a bivalent lectin with monovalent ligands immobilized on a surface: "1 : 1 interaction", "chelating" effect, "proximity/statistical" effect and "clustering" effect.

Département de Chimie Moléculaire - Equipe Ingénierie et Interactions BioMoléculaires, UMR-5250, ICMG FR-2607, CNRS, Université Joseph Fourier - BP 53, 38 041 GRENOBLE cedex 9, France. E-mail: pierre.labbe@ujf-grenoble.fr, angeline.van-der_heyden@ujf-grenoble.fr; Fax: 0 (33) 4 76 51 42 67; Tel: 0 (33) 4 76 51 47 18

† Electronic Supplementary Information (ESI) available: Characterization of the grafting of thiolated RAFT ligands onto gold surfaces. Con A interactions with RAFT-$(Man)_1$ and RAFT-$(Man)_4$ surfaces studied by QCM-D. Analysis of Con A binding using the rectangular hyperbolic relationship. See http://dx.doi.org/10.1039/b716214f/

chemically addressable domains. This structural feature permits the sequential and regioselective assembly of biomolecule-based ligands ("recognition domains") and biologically functional units ("effector domains").[15,16]

We have demonstrated recently that clusters of carbohydrate-based ligands presented at the surface of RAFT molecules ensure the specific recognition and a significantly enhanced affinity for lectins through multivalent interactions in solution[11] and on solid supports.[17,18] It is important to notice that since the distance between two mannose residues of this low-molecular weight tetramannosyl glycoconjugate (~25 Å, as estimated from molecular modeling) is much lower than the distance between two binding sites of Con A (~65 Å),[19] simultaneous binding to multiple sites on the same lectin (chelating effect, Fig. 1A) can be ruled out. Thus, only two effects, *i.e.* proximity/statistical effects and/or lectin clustering could *a priori* explain the observed enhanced affinity. It is important to note that additional phenomena coupled to chelating and/or clustering effects could also occur. Brewer *et al.* have reported that, in solution, Con A binding to multivalent ligands depends on the degree of occupancy with negative cooperativity,[20,21] while positive forces between lectins adsorbed on sugar surfaces were evidenced by Kiessling *et al.*[22] These latter phenomena will not be developed in the following discussion.

On solid supports, binding tests between horseradish peroxidase (HRP) labelled lectins and beads of resin derivatized with neo-glycopeptides displaying clustered lactose, *N*-acetylgalactose and mannose residues have qualitatively shown specific recognition and enhanced affinity through multivalent interactions.[17] Similar conclusions could be obtained with glycopeptide–oligonucleotide conjugates bearing a glycocluster by using microtiter plate binding assays with HRP-labelled lectins.[18] Since presentation at a solid surface is formally multivalent for any system, even with immobilized monovalent ligands, the enhancement obtained with our immobilized multiple carbohydrate-based ligands emphasizes that it is not only the multiple presentation of the sugar ligands that is important for improving the interaction, but also that the control of their local density is crucial. While some papers report systematic studies concerning the impact of the density of monovalent carbohydrate modified surfaces on lectin recognition,[22–29] to our knowledge, only a few examples of lectin–carbohydrate recognition investigated as a function of the grafting ratio of multivalent carbohydrate ligands can be found in literature.[30]

In order to get deeper insights into this recognition process between multivalent immobilized ligands and a model lectin (Con A), we have designed and synthesized RAFT molecules displaying both clusters of sugars and anchoring elements for streptavidin or gold surfaces (Fig. 2). The RAFT molecules bearing four mannose or four lactose moieties (RAFT-$(Man)_4$ and RAFT-$(Lac)_4$ respectively) were synthesized by using a convergent and chemoselective oxime bond strategy.[17] To assess the multivalent effect of such interactions, we also prepared the corresponding monovalent glycopeptides as controls (RAFT-$(Man)_1$ and RAFT-$(Lac)_1$ respectively). As schematically depicted in Fig. 1, the situation is rather complex when ligands are immobilized on a surface. At a high RAFT-$(Man)_4$ surface density (Fig. 1B), the chelating effect induced by the surface presentation cannot be dissociated from the local multivalent effects induced by the RAFT-$(Man)_4$ ligands (proximity/statistical effects or lectin clustering effects). At a sufficiently low RAFT-$(Man)_4$ surface

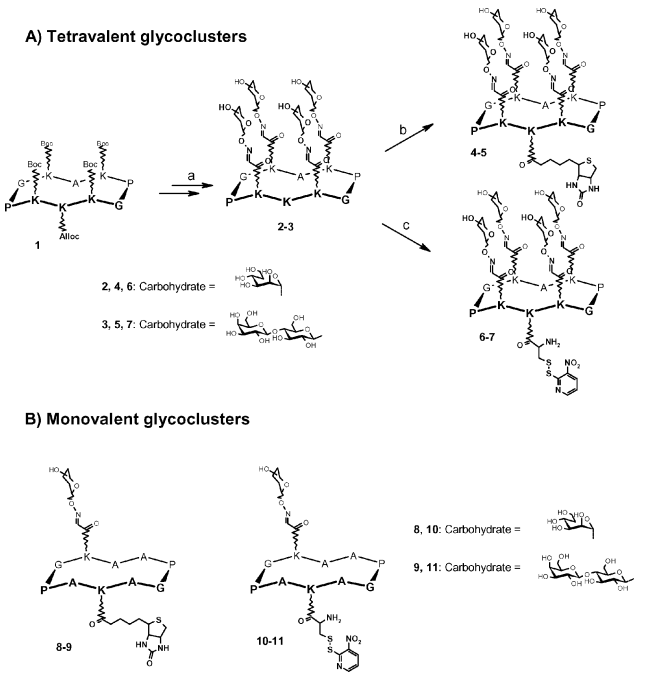

Fig. 2 Synthesis of tetravalent (A) and monovalent (B) glycoclusters. *Reagents and conditions:* (a) See reference;[18] (b) biotin-OSu, DIEA, DMF; (c) i: BocCys(NPys)–OSu, DIEA, DMF; ii: TFA–CH_2Cl_2. In order to facilitate the reading of the manuscript, molecules **2**, **4**, **6** are called RAFT-$(Man)_4$, molecules **8**, **10** are named RAFT-$(Man)_1$. In the same manner, molecules **3**, **5**, **7** are called RAFT-$(Lac)_4$ and molecules **9**, **11** are named RAFT-$(Lac)_1$.

density, the mean distance between adjacent ligands is expected to become larger than the distance between two binding sites of the same lectin, thus allowing suppression of the chelating effect and simplifying the overall system. Similarly, only at a sufficiently low RAFT-$(Man)_1$ surface density, is a monovalent 1 : 1 interaction with Con A expected to occur without the complexity induced by the chelating effect and the statistical/proximity effect (Fig. 1C). For these reasons, we have investigated the Con A binding properties at various RAFT-mannose surface densities by diluting them with RAFT-$(Lac)_4$ ligands which do not interact with the protein. Two complementary real-time techniques, quartz crystal microbalance with energy dissipation monitoring (QCM-D) and surface plasmon resonance (SPR), were employed to investigate the binding processes.

Results

Synthesis

The RAFT molecule **1** (Fig. 2) was prepared following the previously reported protocol.[31] A linear decapeptide was first synthesized on solid phase following the standard Fmoc–*t*Bu strategy using a parallel peptide synthesizer, then cyclized in solution to give the orthogonally protected cyclodecapeptide **1**. After coupling serine moieties to the upper face of the template, followed by acidolysis of protecting groups then generation of aldehyde functions by periodate oxidation, aminooxylated mannose and lactose[32] ligands were introduced as glycoclusters **2** and **3** through oxime linkages.

To ensure the further immobilization of these molecules on streptavidin coated surfaces, we used an active ester to introduce biotin on the side chain of the lysine pointing from the lower face of the molecules **2** and **3**. This reaction occurred in DMF at basic pH to give biotinylated compounds **4** and **5** in good yields after reverse-phase HPLC purification (RP-HPLC).

As a more direct immobilization strategy, we functionalized the compounds **2** and **3** with a cysteine residue bearing the activating group *S*-3-nitro-2-pyridinesulfenyl (Npys) on the side chain. BocCys(Npys) was coupled to the free lysine as the succinic ester in DMF. After removal of the Boc group by treatment with TFA solution and RP-HPLC purification we obtained **6** and **7** which could be readily immobilised on gold surfaces.

QCM-D experiments

QCM-D measures absolute areal mass density (ng cm^{-2}) without the need for a reference channel and with a typical mass sensitivity of 3.5 ng cm^{-2}. RAFT self-assembled monolayers (SAMs) exhibiting variable densities of mannose residues were prepared outside the measurement chamber, by adsorption from 0.1 mM aqueous solutions of RAFT-$(Man)_1$ (ligand **10**) or RAFT-$(Man)_4$ (ligand **6**) diluted with RAFT-$(Lac)_4$ (ligand **7**) at RAFT-mannose : RAFT-$(Lac)_4$ molar ratios of 100, 33, 20, 10, 5 and 2%. A cleaned gold QCM-D sensor was immersed overnight in the RAFT solution, rinsed by milliQ water and dried by nitrogen.[33,34] The surface densities mentioned in the text correspond to the RAFT-mannose bulk concentrations of the solutions used for adsorption. Finally, the functionalized gold-coated quartz was set up in the measurement chamber. 0.005% P20 was added to the working buffer (WB) to prevent non-specific adhesion. No adhesion was observed during a 1μM peanut agglutinin (PNA, a lectin non-specific for mannose) injection onto a 100% RAFT-$(Man)_4$ SAM, confirming the efficiency of the P20 use. *Ex situ* ellipsometry measurements were performed on the gold coated quartz crystal before and after the RAFT immobilization (see ESI†) and gave for the dried RAFT layer an average thickness of 2.1 nm, in agreement with the molecular modeling study (2.5 nm). An *in situ* kinetic study of the RAFT self-assembled monolayer formation was performed by QCM-D (see ESI†). Results confirm that SAM formation is a slow process that needs ~15 hours. Since RAFT immobilization on gold coated quartz offers the ability of surface regeneration, cyclic adsorptions–desorptions of Con A lectin were performed at increasing concentrations on the different SAMs. Each protein adsorption–desorption cycle was followed by two regeneration steps, firstly with a highly concentrated mannose solution (25 mM) and then with a 0.05% SDS solution. Indeed, mannose injections, even at a 50 mM mannose concentration, did not procure a total regeneration of the surface. A representation of a single experiment conducted on a 100% RAFT-$(Man)_4$ surface is shown in Fig. 3.

Con A interactions with RAFT-$(Man)_1$ and RAFT-$(Man)_4$ were compared by overlaying part of the curves concerning each adsorption–desorption cycle of Con A for the same SAM (Fig. ESI-3†). Since the dissipation factor remains low (less than 10^{-6}) for adsorption of the protein, we considered as a first approximation a rigid behaviour for the Con A layer so that the normalized frequency shifts can be linearly related to mass uptake using the Sauerbrey equation. In order to compare the Con A adsorption on the different surfaces, maximum mass uptakes recorded after 9 min of association have been plotted as a function of Con A concentration (Fig. 4).

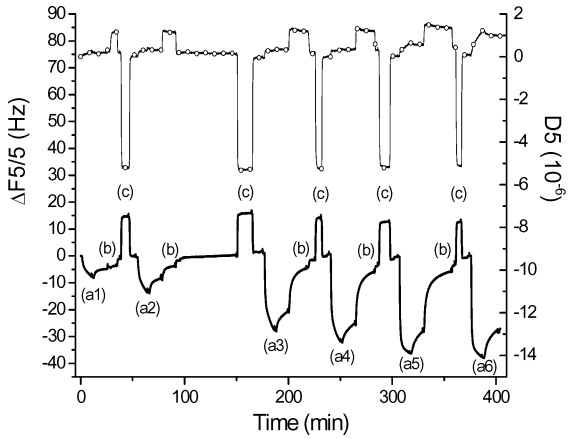

Fig. 3 Typical QCM-D response, normalized frequency $\Delta f_n/n$ (bold line) and D_n variation (thin line) for the third overtones ($n = 3$), recorded during Con A adsorption onto a surface prepared by adsorption of a 100% RAFT-$(Man)_4$ solution. (a) Lectin adsorption (a1) 0.049 μM, (a2) 0.098 μM, (a3) 0.49 μM, (a4) 0.98 μM, (a5) 4.9 μM and (a6) 9.8 μM. The injection of buffer leads to partial dissociation of Con A. Surface regeneration is performed by successive injection of (b) 25 mM mannose solution and (c) 0.05% SDS. The experiments were performed in flow mode at 100 μL min^{-1}.

For both RAFT-mannose saturated surfaces, similar maximum areal mass uptakes of about 710 ng cm^{-2} are obtained upon Con A binding. It is interesting to compare this value with a theoretical mass value calculated for a hydrated Con A monolayer. Assuming a density for the Con A monolayer of ~1.165 g cm^{-3} and considering the hydrated Con A as a cube with edge ~65 Å,[35,36] a theoretical mass of ~770 ng cm^{-2} is obtained. The maximum mass uptake extracted from the QCM-D data agrees well with the theoretical mass. Clearly the mannose surface density exhibited by both kinds of surfaces is enough to ensure the formation of a hydrated Con A monolayer and provides enough sugar heads to complete a multivalent adhesion of the protein.

Differences between the two surfaces are highlighted for higher dilutions of RAFT-mannose in the SAMs. For equivalent dilutions of RAFT-mannose, larger mass uptakes are observed for RAFT-$(Man)_4$ surfaces compared to RAFT-$(Man)_1$ ones, meaning that more protein is adsorbed onto RAFT-$(Man)_4$ SAMs. By increasing the RAFT-mannose dilution in the SAM, distances between ligands on the surface increase and protein binding *via* more than one RAFT-mannose should be avoided. In this case, the chelating effect involved by the surface (Fig. 1) should be progressively removed to the benefit of the local ligand concentration effect (clustering or proximity/statistical effects). However, while a RAFT-$(Man)_4$ molecule benefits more from a higher proximity/statistical effect when binding to one protein than does a RAFT-$(Man)_1$ molecule, this effect could not explain the significantly higher amount of protein adsorbed onto the RAFT-$(Man)_4$ surfaces. It could then be supposed that even if the distance between two sugars on the RAFT scaffold is about 2.5 nm, a RAFT-$(Man)_4$ molecule allows the immobilization of several different Con A. More quantitative information is difficult to extract from these QCM-D experiments for the following reasons.

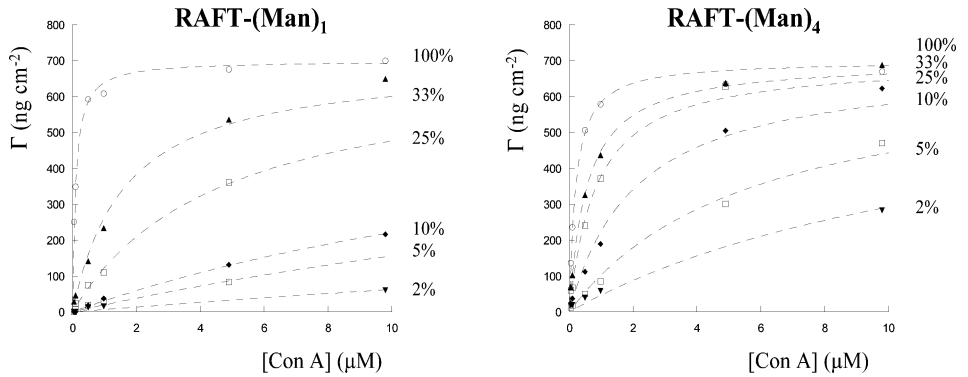

Fig. 4 Maximum mass uptake recorded for Con A binding onto (A) RAFT-$(Man)_1$ and (B) RAFT-$(Man)_4$ adsorbed on gold surfaces. The dotted lines have been drawn for better visualization. The numbers indicate the RAFT-mannose molar ratio of the solutions used for adsorption. Other experimental conditions are reported in the caption for Fig. 3.

Firstly the mass uptake measured by QCM-D includes, in addition to the mass of dry protein, a contribution due to acoustically coupled water. Both contributions (dry protein and coupled water) are not linearly linked. Reliable kinetic or thermodynamic information cannot be deduced since only the amount of adsorbed protein is relevant for this kind of data treatment. Secondly, the association curves of Con A (Fig. ESI-3†) present linear portions that are characteristic of mass transport limitations. Although the present QCM-D experiments were conducted under flowing conditions, both the large measuring chamber volume (~80 μL) and the low flow rate (100 μL min^{-1}) lead to mass transport limitations. For these reasons, SPR experiments based on Biacore technology were realized.

SPR experiments

SAMs exhibiting various sugar dilutions were realized by adsorption from solutions of thiolated RAFT-mannose diluted to the desired ratio with thiolated RAFT-$(Lac)_4$ (Fig. 2). Cleaned gold chips are activated by two injections of 70% ethanol solution. Then various 0.1 mM RAFT solutions in WB are injected during 20 minutes at 5 μL min^{-1}.[37] A 100% RAFT-$(Lac)_4$ SAM is used as a reference. Kinetics curves recorded on this surface reveal a non-specific adhesion of Con A (from 24.5 nM to 39.2 μM) even in the presence of 0.05% of P20 in the working buffer. An increase in the concentration of the thiolated RAFT solution to 1 mM, an increase of contact time between the gold surface and the RAFT solutions to 1 hour, as well as a bovine serum albumin injection prior to the lectin injection were also tested unsuccessfully. Since this problem was not observed with QCM-D experiments, an explanation could be that the contact time between the thiolated molecules and the gold surface (20 min) during a functionalization directly in the SPR sensor chamber is too short compared to the *ex situ* immobilization (15 hours) performed for the QCM-D experiments. As a consequence, only a partial coverage of the gold surface by thiolated RAFT molecules is obtained whereas the remaining free gold surface is expected to induce a strong non-specific Con A adhesion. It could be remarked that while a 15 hour *ex situ* immobilization of thiolated RAFT on a gold sensor chip surface is possible, it will lead to the same functionalization of the four Biacore microchannels. In consequence, no reference surface will be available to exploit the kinetics recorded by the Biacore system. *In situ* functionalization of each of the four Biacore channels could not be realized because it would have needed such a large amount of thiolated RAFT molecules, which was incompatible with the available quantities.

To overcome these difficulties, the four Biacore channels were selectively functionalized with biotinylated RAFT molecules by the way of biotin–streptavidin links. Streptavidin was, firstly, grafted to a C1 carboxylated surface using a classical amine coupling. A similar quantity of streptavidin, ~370 RU, was grafted onto each flow cell, in order to guarantee the same number of available biotin binding sites and the anchoring of a reproducible RAFT surface. The mass uptake Δm_{SPR} can be obtained from relation (1) with C_{SPR} calibrated to ~0.066 ng cm^{-2} for protein adsorption on a flat gold surface.[38]

$$\Delta m_{SPR} = d\frac{n^{eff}_{biomolecule} - n_{buffer}}{dn/dc} = C_{SPR}\Delta RU \qquad (1)$$

The amount of grafted streptavidin was thus estimated to be ~24.5 ng cm^{-2}, which is about 10% of a monolayer.[39] This low grafting level was chosen in order to minimize mass transport limitation during SPR kinetic experiments and to dilute RAFT-mannose on the surface. Anchoring of biotinylated RAFT was then performed by 3 min injection of 5 μM RAFT solutions in WB, at 5 μL min^{-1}. Surfaces exhibiting various RAFT-$(Man)_1$ (ligand **8**) or RAFT-$(Man)_4$ (ligand **4**) densities were prepared by adsorption of RAFT-mannose–RAFT-$(Lac)_4$ (ligand **5**) mixtures obtained by dilution of RAFT-mannose solutions with RAFT-$(Lac)_4$ solution to the desired molar ratio (100%, 25%, 10% and 5%). As for the QCM-D study, the surface densities mentioned in the text correspond to the RAFT–mannose bulk concentrations of the solutions used for adsorption. A surface coated only with RAFT-$(Lac)_4$ was tested and used as a reference. After Con A binding, the RAFT-mannose surfaces could be regenerated by injecting a 50 mM mannose solution. Similar sensorgrams were recorded at various flow rates, which demonstrates the absence of mass transfer limitations (not shown). Fig. 5 compares the binding curves of Con A, recorded at 25 μL min^{-1}, onto surfaces exhibiting various surface densities of RAFT-$(Man)_4$ and RAFT-$(Man)_1$. As already observed by QCM-D, the amount of bound Con A is systematically higher on the RAFT-$(Man)_4$ surfaces, whatever the RAFT-mannose surface density is. Another important difference occurs in the rate of the Con A association–dissociation process,

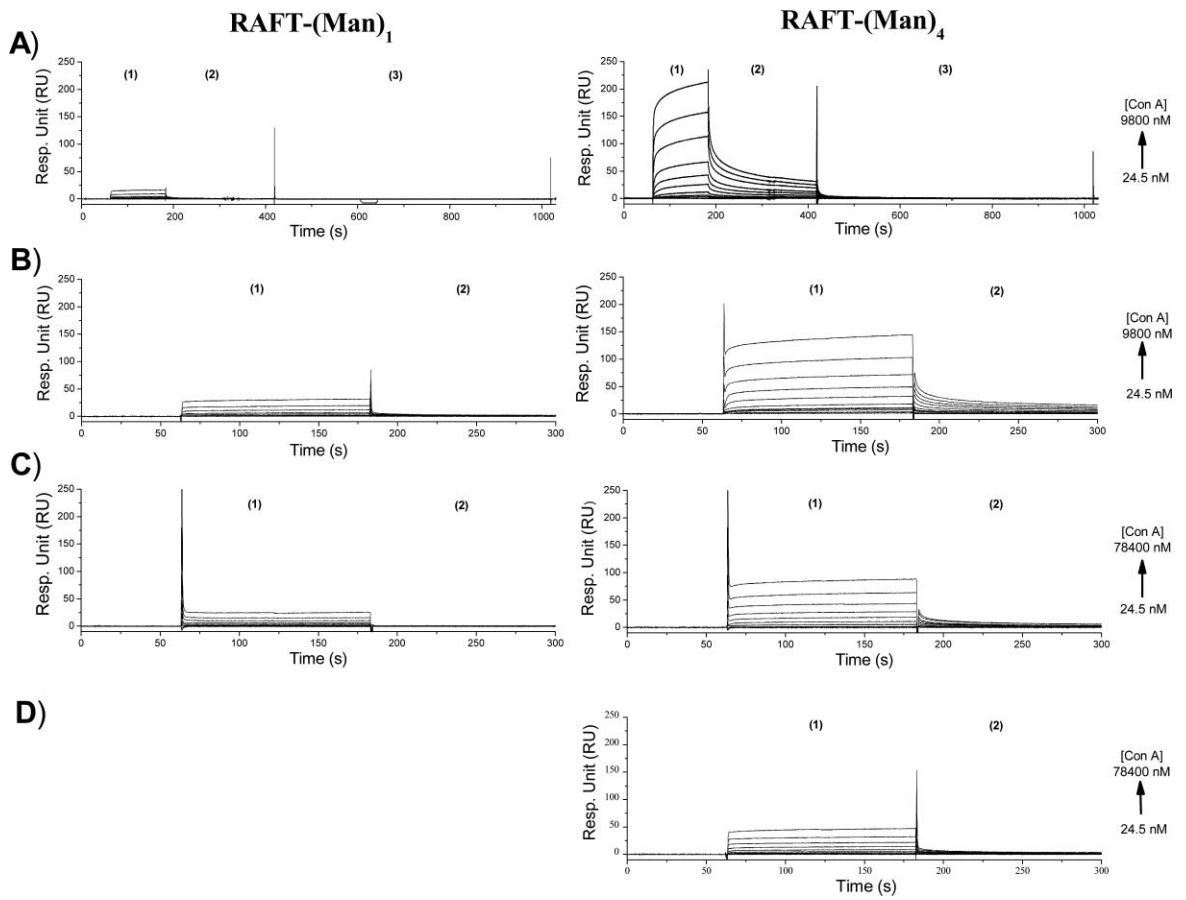

Fig. 5 Comparison of the sensorgrams recorded at 25 μL min^{-1} on RAFT-$(Man)_4$ (right) and RAFT-$(Man)_1$ (left) surfaces. The reference surface is a 100% RAFT-$(Lac)_4$. The RAFT-mannose surfaces were prepared by adsorption of mixed solutions of RAFT-mannose–RAFT-$(Lac)_4$ on streptavidin surfaces. The RAFT-mannose molar ratios of the adsorption solutions are (A) 100% (B) 25% (C) 10% and (D) 5%. At 5% dilution, only the signal recorded on the RAFT-$(Man)_4$ surface is detectable.

which is much more rapid on the RAFT-$(Man)_1$ surfaces than on the RAFT-$(Man)_4$ ones. The responses obtained at equilibrium (R_{eq}) have been considered first. At the lowest RAFT-$(Man)_1$ surface density (10%), a linear Scatchard plot (R_{eq}/C as a function of R_{eq}, with C = [Con A]) is obtained (Fig. 6A). It can thus be concluded that at this dilution, the mean distance between immobilized RAFT-$(Man)_1$ is large enough to avoid a multivalent interaction of Con A with the surface immobilized mannose (chelating effect, Fig. 1C) and that a true monovalent 1 : 1 interaction is observed as expected. From this linear Scatchard plot, a dissociation constant K_D of 110 μM was extracted, which is in good agreement with the values reported in the literature for the interaction of monomeric mannose with Con A.[22]

At higher RAFT-$(Man)_1$ surface densities (25% and 100%), non-linear Scatchard plots were obtained (Fig. 6A) meaning that the interaction cannot be described as a simple 1 : 1 mechanism. As depicted in Fig. 1C, a multivalent interaction of Con A with the RAFT-$(Man)_1$ surface (chelating effect) can explain this deviation. For surfaces modified by RAFT-$(Man)_4$, non-linear Scatchard plots were systematically obtained (Fig. 6B), meaning that, even at the lowest dilution used, a simple monovalent 1 : 1 interaction is never obtained. In this case, a more complex situation is obtained since both the chelating and the clustering effects (Fig. 1B) can be at the origin of this behavior.

Discussion

Our first objective was to rationalize how the presentation of multiple mannose epitopes offered by RAFT scaffolds increases their Con A binding activities relative to their monovalent counterparts. For this purpose, RAFT ligands have been immobilized on gold surfaces at various surface densities, and the binding affinity of Con A towards the resulting surfaces has been assessed using QCM-D and SPR. Since QCM-D allows absolute areal mass determination without needing a reference channel, *ex situ* functionalization of the gold surface transducer is possible by way of self-assembled monolayers of thiolated RAFT. This approach allowed us to prepare surfaces that were fully saturated by RAFT-$(Man)_1$ or RAFT-$(Man)_4$ ligands. Both kinds of these saturated surfaces were able to bind a similar monolayer of Con A, meaning that at high RAFT surface densities, the multiple presentation of mannose does not improve, as expected, the binding activity. It is only at lower surface densities that different behaviors appear between monovalent and multiple ligands. This work has also

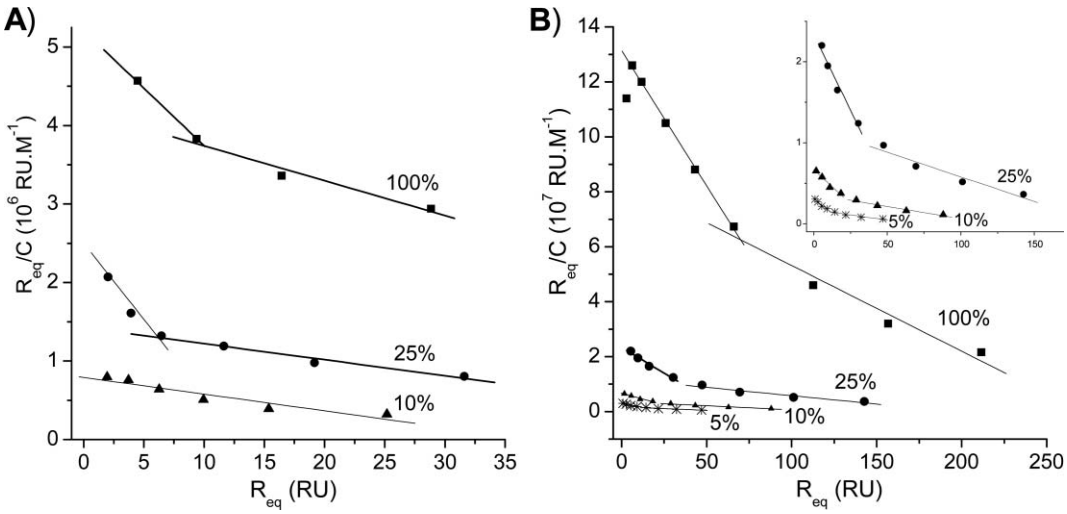

Fig. 6 Scatchard plots of the interaction of Con A with increasing surface densities of (A) RAFT-$(Man)_1$ and (B) RAFT-$(Man)_4$. The numbers indicate the RAFT-mannose molar ratio of the solutions used for adsorption. Insert: part of graph (B) enlarged. Experimental conditions as in Fig. 5.

Table 1 Intrinsic dissociation constant (K_{DX}) and effective concentration (C_X*) of affinity binding sites for the interaction of Con A with RAFT-mannose molecules immobilized at various surface densities. These values are obtained by analyzing the amount of bound Con A on the basis of the modified rectangular hyperbolic relationship with $f = 2$

RAFT-$(Man)_1$	K_{DX}/μM	C_X*/μM	r	RAFT-$(Man)_4$	K_{DX}/μM	C_X*/μM	r
100%	45	0.023	0.9993	100%	6.6	0.067	0.9972
25%	105	0.018	0.9987	25%	34	0.049	0.9960
10%	154	0.012	0.9970	10%	68	0.030	0.9970
				5%	84	0.017	0.9966

pointed out the limitations of QCM-D for these kinds of binding studies. Since QCM-D is sensitive not only to the mass of protein but also to the mass of water that is acoustically coupled with the protein layer, only qualitative results can be obtained by this technique. As a consequence of the design of the QCM-D measuring chamber, mass transport limitations also constitute an important parameter that should be taken into account for any kinetic studies.

Since SPR is only sensitive to the local change in refractive index of a thin layer of liquid in proximity to the transducing surface, the true amount of binding protein can be determined independently of the coupled water. The disadvantage lies in the need to subtract the signal of a reference channel (where binding of the protein does not occur) in order to abstract the refractive index change of the protein solution with regards to the pure buffer. As a consequence, surface functionalization of the different Biacore measuring microchannels must be realized *in situ*, which in our case prohibits the use of thiolated RAFT.

On the other hand, the covalent binding of streptavidin on a C1 sensorchip provided an excellent platform for assessing the binding affinity of Con A for various ligands immobilized on the surface through biotin–streptavidin bridges. In particular, using a low surface density of immobilized streptavidin (~10% of a monolayer[39]) and a high dilution (10%) of the biotinylated RAFT-$(Man)_1$ with RAFT-$(Lac)_4$ provided a surface where only 1 : 1 interactions occurred between immobilized RAFT-$(Man)_1$ and Con A in solution. In agreement with the literature, we found a weak binding affinity ($K_D = 110$ μM) for the monovalent RAFT-$(Man)_1$–Con A interaction. When the RAFT-$(Man)_1$ surface density was increased up to 25% and 100% of the available streptavidin binding sites, larger equilibrium amounts of bound Con A and non-linear Scatchard plots were obtained (Fig. 6A). This was interpreted by multivalent interactions of Con A with the surface (chelating effect, Fig. 1C). Using a modified rectangular hyperbolic relationship, Winzor and co-workers have reported a method for determining an intrinsic dissociation constant (K_{DX}) and an effective concentration of binding sites (C_X*) on a surface for the multivalent interaction of a protein having f equivalent and independent binding sites.[40] From the raw SPR data, a plot of effective bound surface concentration *versus* the effective injected concentration of Con A was generated (see ESI†) from which K_{DX} and C_X* could be extracted (Table 1).

In the case of RAFT-$(Man)_1$ surfaces, it is first interesting to observe that the modified rectangular hyperbolic relationship, used here for a bivalent interaction of Con A (chelating effect with $f = 2$), allows an excellent fitting of the experimental data with high correlation coefficients. As the RAFT-$(Man)_1$ surface density increases, the number of available binding sites and the affinity increase (C_X* increases and K_{DX} decreases). Since it was demonstrated previously that at low RAFT-$(Man)_1$ surface density (10%), the interaction was monovalent, this bivalent Scatchard analysis appears meaningful only at higher RAFT-$(Man)_1$ densities (25% and 100%). In the case of RAFT-$(Man)_4$ surfaces, excellent data fitting is also observed. However in this case, the bivalent Scatchard analysis does not constitute a perfect theoretical model, since in addition to the chelating effect (that is only described by this model), some Con A clustering can occur as a consequence of the multiple mannose presentation

provided by RAFT-$(Man)_4$ molecules. Indeed we observed that, as the RAFT-$(Man)_4$ surface density increases, the affinity increases, but with K_{DX} values that are systematically lower than those observed with RAFT-$(Man)_1$ (Table 1). Another important point is that the amount of available binding sites (C_X*) is systematically higher (by a ratio of about 2.5–3) on RAFT-$(Man)_4$ surfaces (Table 1). Even at a similar mannose surface density but different spatial organization (comparison of 100% RAFT-$(Man)_1$ and 25% RAFT-$(Man)_4$) a better affinity is obtained for RAFT-$(Man)_4$ as compared to RAFT-$(Man)_1$ surfaces (K_{DX} = 34 μM and 45 μM respectively) as well as a higher amount of binding sites (C_X* = 0.048 μM and 0.023 μM respectively). This qualitative analysis strongly suggests that a clustering of Con A can occur on immobilized RAFT-$(Man)_4$, which greatly improves both the affinity, by a factor of 3 to 7, and increases the number of binding sites by a factor of about 3.

To confirm the ability of RAFT-$(Man)_4$ molecules to bind two or more proteins, a competitive binding experiment was conducted and followed by SPR. Solutions of Con A (16.33 μM) mixed with various quantities of RAFT-$(Man)_1$ or RAFT-$(Man)_4$ were injected onto the 100% RAFT-$(Man)_1$ surface prepared *via* streptavidin–biotin interaction as described previously. The responses obtained at the end of the association time as a function of the RAFT-mannose concentration in solution are presented in Fig. 7.

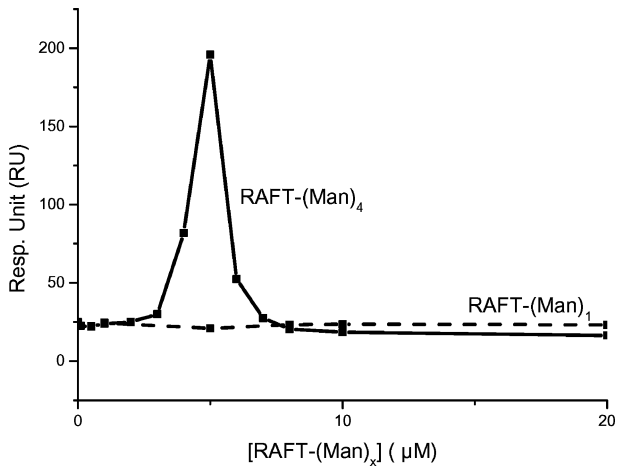

Fig. 7 SPR response recorded for the association of Con A (16.33 μM) with 100% RAFT-$(Man)_1$ surfaces obtained through biotin-streptavidin bridges in the presence of increasing concentrations of RAFT-$(Man)_4$ (solid line) or RAFT-$(Man)_1$ (dashed line).

No signal variations are observed for injection of Con A in the presence of RAFT-$(Man)_1$ meaning that this monovalent molecule is not able, within the range of concentrations explored, to compete efficiently with the binding affinity of Con A towards the multivalent mannosylated surface. On the opposite hand, a large signal enhancement is observed for Con A injected in the presence of 3 to 6 μM of RAFT-$(Man)_4$, with a maximum response recorded for 5 μM. Thus, tetravalent RAFT-$(Man)_4$ appears to effectively bind and promote the clustering of Con A in solution at concentrations where no inhibition by monovalent RAFT-$(Man)_1$ is observed. It could be supposed that in the bulk phase, RAFT-$(Man)_4$ binds at least two or three lectins to form soluble clusters.[5] These clusters could then interact with the RAFT-$(Man)_1$ surfaces. In this range of concentrations, RAFT-$(Man)_4$ behaves as a promoter of the Con A–RAFT-$(Man)_1$ surface interaction since Con A aggregates exhibit a more important multivalent behavior. For higher RAFT-$(Man)_4$ concentrations, inhibition of the interaction between Con A and the RAFT-$(Man)_1$ surface is observed as expected. Whereas Con A presents four sugar-binding sites, inhibition occurs at a RAFT-$(Man)_4$–Con A molar ratio closer to 1. Probably the lectins are too aggregated to exhibit free binding sites to the surface.

Conclusion

Tetravalent carbohydrate-based ligands presented at the surface of cyclodecapeptidic RAFT scaffolds cannot span the saccharide binding sites within the same Con A tetramer. In solution, these multivalent ligands have been found to promote the formation of Con A clusters that exhibit enhanced affinity toward carbohydrate-substituted surfaces. When immobilized on a surface at various surface densities, these multivalent ligands exhibit affinities towards Con A that are typically 3 to 7 fold better than their monovalent counterpart. At similar surface densities they can bind about 3-fold higher amounts of Con A as a consequence of their ability to form clusters of lectins. This lectin clustering process could be at the origin of the higher affinity exhibited by the multivalent ligands, although the presence of a high local concentration could also participate through a proximity/statistical effect. Complementary work is in progress to quantify the relative influence of these two processes.

Experimental

Synthesis

All chemical reagents and solvents were purchased from Sigma Aldrich, Acros or Carlo-Erba and were used without further purification. All protected amino acids were obtained from Advanced ChemTech Europe (Brussels, Belgium), Bachem Biochimie SARL (Voivins-Le-Bretonneux, France) and France Biochem S.A. (Meudon, France). Fmoc-Gly-SASRIN® resin was purchased from Bachem and PyBOP from France Biochem. Reverse phase HPLC analyses were performed on Waters equipment: the analytical (Nucleosil 120 Å 3 μm C_{18} particles, 30 × 4.6 mm) was operated at 1.3 mL min^{-1} and the preparative (Delta-Pak 300 Å 15 μm C_{18} particles, 200 × 25 mm) at 22 mL min^{-1} with UV monitoring at 214 nm and 250 nm using a linear A–B gradient (buffer A: 0.09% CF_3CO_2H in water; buffer B: 0.09% CF_3CO_2H in 90% acetonitrile). Mass spectra were obtained by electron spray ionization (ES-MS) on a VG Platform II in the positive mode.

Synthesis of tetravalent neoglycopeptides 2 and 3

Aminooxy α-D-mannopyranosyl (28 mg, 144 μmol) or β-D-lactopyranoyl (109 mg, 305 μmol)[32] was added to a solution of RAFT molecule bearing aldehyde functions (18 mg, 14.4 μmol for mannose; 38 mg, 30.5 μmol for lactose) in 20% aqueous acetic acid (1 mL). After stirring for 3 hours at room temperature, compounds **2** (20 mg, 71%) and **3** (46 mg, 59%) were purified by semi-preparative RP-HPLC (linear gradient: 95 : 5 to 60 : 40 A : B in 30 min, detection: λ = 214 and 250 nm). Compound **2**: R_t = 7.3 min (linear gradient: 95 : 5 to 60 : 40 A : B in 15 min);

ES-MS (positive mode): calcd for $C_{79}H_{130}N_{19}O_{38}$ 1952.88 $[M + H]^+$, found: 1953.09; compound **3**: $R_t = 6.6$ min (linear gradient: 95 : 5 to 60 : 40 A : B in 15 min); ES-MS (positive mode): calcd for $C_{103}H_{169}N_{19}O_{58}Na$ 2623.07 $[M + Na]^+$, found: 2622.86.

Synthesis of biotin functionalized tetravalent neoglycopeptides 4 and 5

Neoglycopeptide **2** (7 mg, 3.6 mmol) and biotin-OSu (2.5 mg, 7.2 mmol) were dissolved in DMF (1 mL) and the pH of the solution adjusted to 8 with DIEA. After 30 minutes at room temperature and purification by semi-preparative RP-HPLC (linear gradient: 95 : 5 to 60 : 40 A : B in 30 min, detection: $\lambda = 214$ and 250 nm), compound **4** (5 mg, 59%) was obtained as a white powder: $R_t =$ 8.8 min (linear gradient: 95 : 5 to 60 : 40 A : B in 15 min); ES-MS (positive mode): calcd for $C_{89}H_{144}N_{21}O_{40}S$ 2178.96 $[M + H]^+$, found: 2178.65. The same procedure was followed for the synthesis of **5**: $R_t = 8.4$ min (linear gradient: 95 : 5 to 60 : 40 A : B in 15 min); ES-MS (positive mode): calcd for $C_{113}H_{184}N_{21}O_{60}S$ 2827.17 $[M + H]^+$, found: 2828.56.

Synthesis of cysteine functionalized tetravalent neoglycopeptides 6 and 7

Neoglycopeptide **2** (5.5 mg, 2.8 mmol) and BocCys(Npys)-OSu (2.6 mg, 5.6 mmol) were dissolved in DMF (1 mL) and the pH of the solution adjusted to 8 with DIEA. After 30 minutes the solvent was evaporated and the peptide precipitated in diethyl ether. The crude yellow powder was then taken up with a solution of TFA–CH_2Cl_2 (1 : 1, 10 mL) and purified by semi-preparative RP-HPLC (linear gradient: 95 : 5 to 60 : 40 A : B in 30 min, detection: $\lambda = 214$ and 250 nm). Compound **6** (4.5 mg, 72%) was obtained as a yellow powder: $R_t = 9.9$ min (linear gradient: 95 : 5 to 60 : 40 A : B in 15 min); ES-MS (positive mode): calcd for $C_{87}H_{137}N_{22}O_{41}S_2$ 2209.87 $[M + H]^+$, found: 2210.93. The same procedure was followed for the synthesis of compound **7**: $R_t = 9.2$ min (linear gradient: 95 : 5 to 60 : 40 A : B in 15 min); ES-MS (positive mode): calcd for $C_{111}H_{177}N_{22}O_{61}S_2$ 2858.08 $[M + H]^+$, found: 2859.50.

Synthesis of biotin functionalized monovalent neoglycopeptides 8 and 9

Compounds **8** and **9** were prepared following the procedure described above for **4** and **5**. Compound **8**: $R_t = 9.2$ min (linear gradient: 95 : 5 to 60 : 40 A : B in 15 min); ES-MS (positive mode): calcd for $C_{56}H_{89}N_{15}O_{19}S$ 1307.62 $[M + H]^+$, found: 1308.09; compound **9**: $R_t = 8.6$ min (linear gradient: 95 : 5 to 60 : 40 A : B in 15 min); ES-MS (positive mode): calcd for $C_{62}H_{100}N_{15}O_{24}S$ 1470.68 $[M + H]^+$, found: 1470.50.

Synthesis of cysteine functionalized monovalent neoglycopeptides 10 and 11

Compound **10** and **11** were prepared following the procedure described above for **6** and **7**. Compound **10**: $R_t = 10.3$ min (linear gradient: 95 : 5 to 60 : 40 A : B in 15 min); ES-MS (positive mode): calcd for $C_{54}H_{83}N_{16}O_{20}S_2$ 1339.54 $[M + H]^+$, found: 1339.60; compound **11**: $R_t = 10.1$ min (linear gradient: 95 : 5 to 60 : 40 A : B in 15 min); ES-MS (positive mode): calcd for $C_{60}H_{93}N_{16}O_{25}S_2$ 1501.59 $[M + H]^+$, found: 1501.62.

Buffer and other chemicals

Concanavalin A (Con A) was purchased from Fluka, streptavidin, bovine serum albumin and peanut agglutinin from Sigma. All other reactants are analytical grade, $CaCl_2$ came from Normapur, anhydrous $MnCl_2$ from Acros organics, sodium dodecyl sulphate (SDS) from Panreac and *N*-(2-hydroxyethyl)piperazine-*N*′-(2-ethanesulfonic acid) (HEPES) from Euromedex. P20 was provided by Biacore.

The working buffer (WB) used for all experiments consisted of HEPES saline buffer (HBS) (0.1 M HEPES, NaCl 0.1 M) pH 7.2 with 1 mM $CaCl_2$ and 1 mM $MnCl_2$.

Substrate preparation

Gold QCM-D sensors and gold-coated glass slides (SIA Au kit, Biacore, Sweden) were treated by exposure to UV–ozone for 10 min followed by immersion in ethanol for 15 min. Then, surfaces were dried with nitrogen and docked in the SPR measurement chamber or, for QCM-D experiments, immersed in the functionalization solution.

QCM-D measurement

Experiments were performed on a quartz crystal microbalance with an energy dissipation Q-SENSE D300 system equipped with a radial flow chamber from Q-sense AB (Västra Frölunda, Sweden). Changes in the resonance frequencies (Δf), related to attached mass (including coupled water), and its dissipation, ΔD, related to frictional (viscous) losses in the adlayer, are measured simultaneously during the assembling process for the quartz crystal fundamental resonance frequency ($f_1 = 5$ MHz) and odd overtones ($n = 3, 5, 7$). In the case of homogeneous, quasi-rigid films with low thickness, the areal adsorbed masses, $\Delta\Gamma$, could be calculated according to the Sauerbrey equation,[41] $\Delta\Gamma = -C\frac{\Delta f_n}{n}$ with the mass sensitivity $C = 17.7$ ng cm^{-2} Hz^{-1} for $f_1 = 5$ MHz.

QCM-D measurements were operated in flow mode (0.1 mL min^{-1}). The T-loop in the measurement chamber was bypassed and all solutions were kept in a thermostated bath (24.5 °C) to ensure stable operation at a working temperature of 24 °C. All solutions were previously degassed in order to avoid bubble formation in the QCM-D measuring chamber.

SPR measurement

The SPR measurements were performed with a BIAcore T100 (Biacore AB, Sweden) operated with BIAcore T100 evaluation software 1.1. All measurements were performed at 25 °C, at 5 μL min^{-1} for ligand immobilization and 25 μL min^{-1} for kinetic measurements. Experiments were realized in WB containing 0.05% P20. The SPR technique detects changes expressed in relative units (RU) in the interfacial effective refractive index resulting from the binding of an analyte in solution to a ligand immobilized on a sensor chip. For all BIAcore experiments, 0.05% P20 in buffer solution was used to prevent non-specific interactions between proteins and the surfaces. A non-specific surface was used as a reference. Curves obtained on the reference surface were subtracted from the curves recorded on the recognition surfaces, allowing elimination of refractive index changes due to buffer effects. The absence of mass transport effects on experiments was

checked on each surface by separately running one injection of Con A (9.8 μM) for 1 min at three different flow rates (5, 15 and 75 μL min^{-1}). The curves obtained are able to be overlaid, confirming the kinetic control of the experiments (not shown).

Ellipsometry

Ellipsometric measurements were performed using an imaging ellipsometer EP^3-SE from Nanofilm Technology GmbH, Germany. Experiments were performed *ex situ* under air conditions at a wavelength of 630.2 nm and at variable angles of incidence ranging from 50° to 80°. Optical modeling was performed using the EP3View software from Nanofilm Technology GmbH. A three-layer model, substrate–layer–ambient air, was used to fit the data. The optical properties of the bare gold substrate (a QCM-D gold coated quartz crystal) were previously measured.

Acknowledgements

The authors thank Eva Pebay-Peyroula for giving us access to the BIAcore 3000 device in the IBS (Institute of Structural Biology, Grenoble, France). They are indebted to Hughes Lortat-Jacob for his introduction to the BIAcore measurements and to Anne Imberty for useful discussions. The authors thank the Institut de Chimie Moléculaire de Grenoble (ICMG FR-2607) for financial support. M.W. acknowledges the Ministère de l'Education Nationale, de l'Enseignement Supérieur et de la Recherche for her Ph.D. fellowship. We are grateful to the Nanobio program for the facilities of the synthesis and surface characterization platforms.

References

1 H. Lis and N. Sharon, *Chem. Rev.*, 1998, **98**, 637–674.
2 R. A. Dwek, *Chem. Rev.*, 1996, **96**, 683–720.
3 Y. C. Lee and R. T. Lee, *Acc. Chem. Res.*, 1995, **28**, 321–327.
4 S.-K. Choi, *Synthetic Multivalent Molecules: Concepts and Biomedical Applications*, John Wiley & Sons, Inc., Hoboken, New Jersey, 2004.
5 S. D. Burke, Q. Zhao, M. C. Schuster and L. L. Kiessling, *J. Am. Chem. Soc.*, 2000, **122**, 4518–4519.
6 L. L. Kiessling, J. E. Gestwicki and L. E. Strong, *Angew. Chem., Int. Ed.*, 2006, **45**, 2348–2368.
7 J. J. Lundquist and E. J. Toone, *Chem. Rev.*, 2002, **102**, 555–578.
8 M. L. Wolfenden and M. J. Cloninger, *Bioconjugate Chem.*, 2006, **17**, 958–966.
9 S. L. Mangold and M. J. Cloninger, *Org. Biomol. Chem.*, 2006, **4**, 2458–2465.
10 D. Boturyn, J.-L. Coll, E. Garanger, M.-C. Favrot and P. Dumy, *J. Am. Chem. Soc.*, 2004, **126**, 5730–5739.
11 O. Renaudet and P. Dumy, *Org. Lett.*, 2003, **5**, 243–246.
12 S. Grigalevicius, S. Chierici, O. Renaudet, R. Lo-Man, E. Deriaud, C. Leclerc and P. Dumy, *Bioconjugate Chem.*, 2005, **16**, 1149–1159.
13 J. Razkin, V. Josserand, D. Boturyn, Z.-h. Jin, P. Dumy, M. Favrot, J.-L. Coll and I. Texier, *ChemMedChem*, 2006, **1**, 1069–1072.
14 M. Mutter, P. Dumy, P. Garrouste, C. Lehmann, M. Mathieu, C. Peggion, S. Peluso, A. Razaname and G. Tuchscherer, *Angew. Chem., Int. Ed. Engl.*, 1996, **35**, 1482–1485.
15 O. Renaudet and P. Dumy, *Bioorg. Med. Chem. Lett.*, 2005, **15**, 3619–3622.
16 E. Garanger, D. Boturyn, O. Renaudet, E. Defrancq and P. Dumy, *J. Org. Chem.*, 2006, **71**, 2402–2410.
17 O. Renaudet and P. Dumy, *Org. Biomol. Chem.*, 2006, **4**, 2628–2636.
18 Y. Singh, O. Renaudet, E. Defrancq and P. Dumy, *Org. Lett.*, 2005, **7**, 1359–1362.
19 U. Bakowsky, W. Rettig, G. Bendas, J. Vogel, H. Bakowsky, C. Harnagea and U. Rothe, *Phys. Chem. Chem. Phys.*, 2000, **2**, 4609–4614.
20 T. K. Dam, R. Roy, D. Page and C. F. Brewer, *Biochemistry*, 2002, **41**, 1351–1358.
21 T. K. Dam, R. Roy, D. Page and C. F. Brewer, *Biochemistry*, 2002, **41**, 1359–1363.
22 E. A. Smith, W. D. Thomas, L. L. Kiessling and R. M. Corn, *J. Am. Chem. Soc.*, 2003, **125**, 6140–6148.
23 J. Shi, T. Yang, S. Kataoka, Y. Zhang, A. J. Diaz and P. S. Cremer, *J. Am. Chem. Soc.*, 2007, **129**, 5954–5961.
24 P. Critchley and G. J. Clarkson, *Org. Biomol. Chem.*, 2003, **1**, 4148–4159.
25 P. Critchley, M. N. Willand, A. K. Rullay and D. H. G. Crout, *Org. Biomol. Chem.*, 2003, **1**, 928–938.
26 D. A. Mann, M. Kanai, D. J. Maly and L. L. Kiessling, *J. Am. Chem. Soc.*, 1998, **120**, 10575–10582.
27 Y. Shinohara, Y. Hasegawa, H. Kaku and N. Shibuya, *Glycobiology*, 1997, **7**, 1201–1208.
28 N. Horan, L. Yan, H. Isobe, G. M. Whitesides and D. Kahne, *Proc. Natl. Acad. Sci. U. S. A.*, 1999, **96**, 11782–11786.
29 E. Duverger, N. Frison, A.-C. Roche and M. Monsigny, *Biochimie*, 2003, **85**, 167–179.
30 Y. Suda, A. Arano, Y. Fukui, S. Koshida, M. Wakao, T. Nishimura, S. Kusumoto and M. Sobel, *Bioconjugate Chem.*, 2006, **17**, 1125–1135.
31 M.-P. Dubois, C. Gondran, O. Renaudet, P. Dumy, H. Driguez, S. Fort and S. Cosnier, *Chem. Commun.*, 2005, 4318–4320.
32 O. Renaudet and P. Dumy, *Tetrahedron Lett.*, 2001, **42**, 7575–7578.
33 J. C. Love, L. A. Estroff, J. K. Kriebel, R. G. Nuzzo and G. M. Whitesides, *Chem. Rev.*, 2005, **105**, 1103–1169.
34 A. Van der Heyden, M. Wilczewski, P. Labbé and R. Auzely, *Chem. Commun.*, 2006, 3220–3222.
35 Z. Derewenda, J. Yariv, J. R. Helliwell, A. J. Kalb, E. J. Dodson, M. Z. Papiz, T. Wan and J. Campbell, *EMBO J.*, 1989, **8**, 2189–2193.
36 J. H. Naismith, C. Emmerich, J. Habash, S. J. Harrop, J. R. Helliwell, W. N. Hunter, J. Raftery, A. J. Kalb and J. Yariv, *Acta Crystallogr., Sect. D: Biol. Crystallogr.*, 1994, **D50**, 847–858.
37 V. Mansuy-Schlick, R. Delage-Mourroux, M. Jouvenot and W. Boireau, *Biosens. Bioelectron.*, 2006, **21**, 1830–1837.
38 S. Löfaas, M. Malmqvist, I. Roennberg, E. Stenberg, B. Liedberg and I. Lundström, *Sens. Actuators, B*, 1991, **B5**, 79–84.
39 C. Larsson, M. Rodahl and F. Höök, *Anal. Chem.*, 2003, **75**, 5080–5087.
40 N. L. Kalinin, L. D. Ward and D. J. Winzor, *Anal. Biochem.*, 1995, **228**, 238–244.
41 G. Sauerbrey, *Z. Phys. A: Hadrons Nucl.*, 1959, **155**, 206–222.

